4th URSI AT-RASC, Gran Canaria, 19-24 May 2024

Gold nanoparticles mediation and fiber optics thermal monitoring for enhanced laser ablation

Elena De Vita* (1), Federica Bianconi(2), Marco Giustra(3), Brian Novati(3), Daniela Lo Presti(2,4), Alessio Gizzi(2), Agostino Iadicicco(1), Lucia Salvioni(3), Carlo Massaroni(2,4), Davide Prosperi(3), Emiliano Schena(2,4), Stefania Campopiano(1)

(1) Department of Engineering, University of Naples "Parthenope", Naples, Italy
(2) Research Unit of Measurements and Biomedical Instrumentation, Department of Engineering, Università Campus Bio-Medico di Roma, Via Alvaro del Portillo 21, 00128 Roma, Italy
(3) Department of Biotechnology and Bioscience, University of Milano Bicocca, Milan, Italy
(4) Fondazione Policlinico Universitario Campus Bio-Medico, Via Alvaro del Portillo, 200, 00128 Roma, Italy

Abstract

The use of nanomaterials in combination with laser ablation represents an advanced approach to cancer therapy. The injection of specific nanoparticles (NPs) into the tumor site, indeed, is able to enhance the localized heating by laser radiation conversion into thermal energy, resulting in more efficient tumor destruction. Simultaneously, temperature monitoring provides feedback about both treatment progress and NPs efficacy, being a valuable tool for enabling real-time adjustments in a clinical scenario based on the thermal distribution within the lesion. This study focuses on the development and testing of novel structures of polymer-coated gold NPs for laser ablation enhancement. Agarose-based phantoms embedding the synthesized NPs have been prepared to perform in-vitro tests and four arrays of fiber Bragg gratings (FBGs) have been positioned inside the phantom in a reproducible configuration in order to accurately monitor the temperature inside the target region. Three kinds of NPs have been tested and compared in terms of induced temperature increase.

1. Introduction

The benefits of laser ablation over conventional surgical resection are numerous: minimally-invasiveness, also with respect to the other thermal ablation techniques, the capability to treat tumors located in critical regions, and reduced hospitalization of the patients [1]. Moreover, integrating nanoparticles (NPs) into the laser ablation process enhances the heating phenomenon by increasing the magnitude of light absorption within the target tissue, offering several advantages in terms of targeted therapy, reduced side effects, and improved outcomes [2]. For these reasons, laser ablation mediated by nanoparticles (NP-LA) represents an innovative and promising approach in the field of cancer therapy.

Besides involving NPs, a further factor able to improve the ablation selectivity lies in temperature feedback, which allows the treatment control in terms of setting adjusting based on the driving parameter, i.e., the temperature distribution inside the lesion during the laser delivery [3,4]. Such feedback, in turn, can help in assessing the effects of the employed NPs and providing information about their efficacy. One of the most promising thermometric techniques for thermal ablation is represented by fiber Bragg gratings (FBGs) for their advantageous properties like minimal invasiveness, biocompatibility, multiplexing capabilities, and fast response [5,6].

Among the available nano-agents, conductive metal NPs like gold and silver ones, act as good mediators for tumor ablation since they exhibit unique photothermal properties that induce surface electrons to interact with the particle nature of light, efficiently absorb laser energy, and convert it into localized heat [7,8]. On this basis, ongoing research is focusing on optimizing NP design by tuning shape, size and chemicals, improving delivery methods, and addressing potential challenges, such as nanoparticle clearance from the body [8–10].

In this work, a novel structure of hollow NPs, i.e., polymer-coated gold nanocages, has been proposed, and three typologies of the same showing different surface plasmon resonance peaks have been tested during in-vitro experiments of NP-LA on agarose-based phantoms. Aiming to compare the developed kinds of NPs, their effects in terms of phantom heating have been measured. Thus, temperature distribution within the target region has been assessed through four arrays of FBGs deployed in the phantom for a total of 34 sensing points inside a narrow volume around the laser applicator.

2. Materials and Methods

To perform in-vitro experiments of laser ablation mediated by nanoparticles (NP-LA), novel structures of gold nanoparticles have been synthesized, and an ad-hoc experimental setup has been developed, as described in the following paragraphs.

2.1 Synthesis of Gold Nanoparticles

Polymer-coated gold nanoparticles, with size distribution below 50 nm, were synthesized using the Xia protocol [11]. The procedure involved employing silver nanocubes obtained through polyol synthesis as substrates for the galvanic replacement method. By varying the amount of $HauCl_4$ added, three distinct types of gold nanocages (NP_1, NP_2, and NP_3) were obtained to achieve specific absorption wavelengths corresponding to their localized surface plasmon resonance. Specifically, NP_1, NP_2, and NP_3 exhibit absorption peaks at 735 nm, 830 nm, and 960 nm, respectively, as shown in Figure 1, reporting the UV-VIS spectra for each of them.

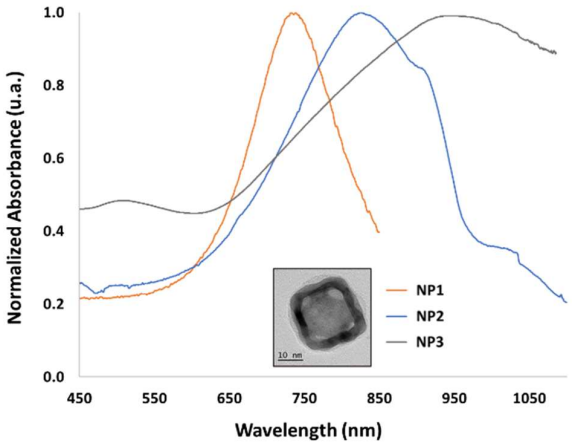

Figure 1. UV-VIS spectra of the synthesized gold NPs.

2.2 Setup for NP-LA Experiments

Figure 2a shows the setup used for performing the NP-LA experiments.

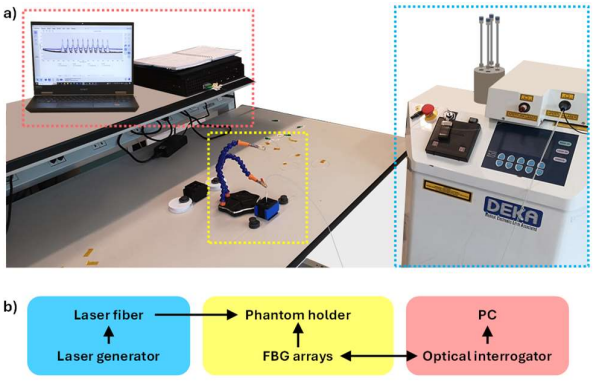

Figure 2. a) Photo of the experimental setup where the dashed red rectangle contains the optical equipment, the yellow one contains the phantom holder, and the blue one the laser instrumentation; b) schematic showing the connections among the components of the experimental setup.

As can be inferred from the picture, the setup can be divided in three main blocks: i) laser instrumentation to deliver the treatment (blue dashed rectangle), ii) phantom holder to shape the phantom and perform reproducible experiments (yellow dashed rectangle), and iii) optoelectronic equipment for performing temperature monitoring (red dashed rectangle).

In particular, laser instrumentation includes a laser generator (Smart 1064 BS DEKA by M.E.L.A. Srl) and the fiber optic laser (quartz optical bare fiber by Asclepion Laser Technologies) working as an applicator. Instead, the holder contains the phantom undergoing the NP-LA which embeds several optical fibers for both laser delivery and temperature monitoring. Inside the phantom, indeed, through dedicated holes of the holder, besides the laser fiber, four more optical fibers, each one embedding an array of Fiber Bragg Gratings (FBGs), are inserted for measuring the temperature in specific points of the phantom during each test. Finally, the optoelectronic equipment used for recording the temperature data measured by the FBGs includes an optical interrogation unit (Hyperion si255 by Micron Optics) and a PC for data displaying and elaboration. The connections among the setup components are shown in Figure 2b.

The structure of the phantom holder is reported more in detail in Figure 3. It is a modular cubic box having dedicated holes for pouring the liquid phantom mixture (in red in Figure 3a), inserting the laser fiber vertically (in light blue in Figure 3a), and inserting the fibers of the FBGs horizontally (in green in Figure 3a).

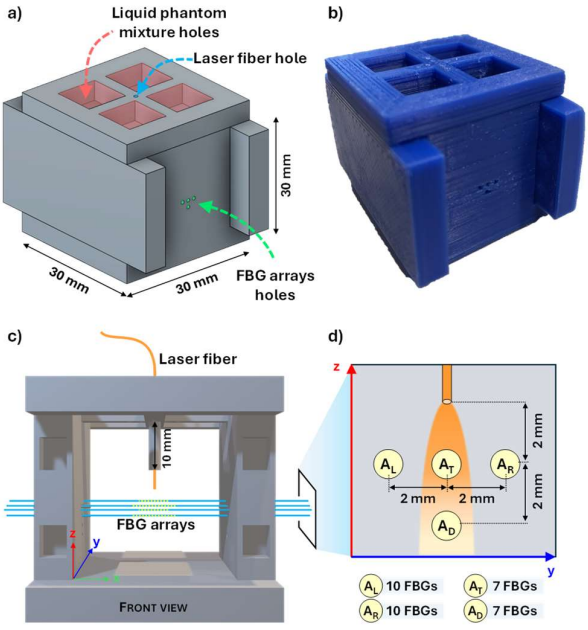

Figure 3. Details of the phantom holder: a) schematic of the holder; b) photo; c) front view of the inside of the phantom; d) zoom showing the spatial configuration of laser tip and FBG arrays in the YZ plane.

Figure 3b reports a photo of the phantom holder, whose elements have been manufactured by using 3D printing,

whereas Figure 3c shows the inside of the holder to clarify the position of the fibers for the FBGs with respect to the laser fiber, the latter being inserted through a guide 10 mm long. As highlighted in Figure 3d, the arrays of FBGs are at 2 mm from each other and the laser tip is at 2 mm from the top central array of FBGs (denoted by A_T). Both A_T and the array below, denoted by A_D, are produced by AtGratings Technologies and embed 10 FBGs, whereas the left and right arrays, denoted by A_L and A_R, respectively, are produced by Technica and embed 7 FBGs each. For all the arrays, FBGs are 1 mm long and separated of 2 mm from each other. It is worth noting that, in order to hold the fibers of the FBGs in position, both ends of the fibers outside the holder were placed between two magnetic disks.

Once positioned the fibers for laser and sensors, the liquid phantom mixture was poured into the holder from the top square holes of the cover. The mixture was prepared by melting agarose powder with a 4% in weight concentration in deionized water and by mixing the NPs at 30 µg/mL. Then, the liquid mixture was left in the holder at room temperature for 1 hour until the solidification of the phantom.

2.3 Working mechanism of FBGs

When a portion of optical fiber core undergoes a periodic modulation of the refractive index, a FBG can be permanently obtained. The peculiarity of such an in-fiber structure is given by the FBG-induced reflection phenomenon, so that when the fiber is illuminated by a broadband spectrum the FBG reflects a narrow range centered around the Bragg wavelength, denoted with λ_B. Such a wavelength shifts in response to variations of temperature and strain from the external environment, making the FBG sensitive to both these physical parameters.
For our experiments, the use of magnetic disks blocking the ends of the fibers of the FBG arrays prevents any mechanical strain, so that the λ_B shift experienced by each FBG, i.e., $\Delta\lambda_B$, only relates to the temperature variation ΔT around the sensor through the following equation [12]:

$$\Delta\lambda_B/\lambda_B = S_T\Delta T \quad (1).$$

where S_T is the thermal sensitivity coefficient of the FBG. During the NP-LA tests, the employed FBG arrays have been interrogated with a sampling frequency of 1 kHz and a wavelength resolution of 1 pm, enabling the temperature detection with a resolution of 0.1 °C.

3 Results and Discussion

The in-vitro experiments of NP-LA have been performed on several phantom samples: from 6 to 12 tests for each type of NPs have been carried out. Regarding the implemented ablation protocol, the power was set at 3 W and the treatment duration at 2 min for each test [13].

Aiming to compare the effects in terms of temperature increment recorded in the ablation volume by the FBG arrays for the different types of synthesized NPs, the ΔT profiles recorded by each FBG during each test for the same kind of NPs have been averaged. The maximum value for each of the averaged ΔT profiles, i.e., ΔT_{max}, is reported in Table I for all the arrays.

Table I. Maximum values of the average temperature variation recorded by each array of FBGs with NP_1, NP_2, and NP_3.

	ΔT_{max} [°C]			
	A_T	**A_D**	**A_L**	**A_R**
NP_1	33.4	25.9	12.9	15.7
NP_2	34.5	20.6	19.0	17.0
NP_3	51.5	44.6	31.4	35.6

As can be inferred from Table I, the temperature increments recorded by the FBG arrays increase passing from NP_1 to NP_2 and, even more, from NP_2 to NP_3. Therefore, tests confirmed that when the absorbing peak of the NPs approaches the laser emitting wavelength, i.e., 1064 nm, their effect increases in terms of phantom heating nearby the laser applicator.

Figure 4 reports the ΔT profiles recorded by each FBG during one of the performed NP-LA tests with NP_3, which resulted the most efficient ones in terms of heating increase, and grouped by the corresponding array.

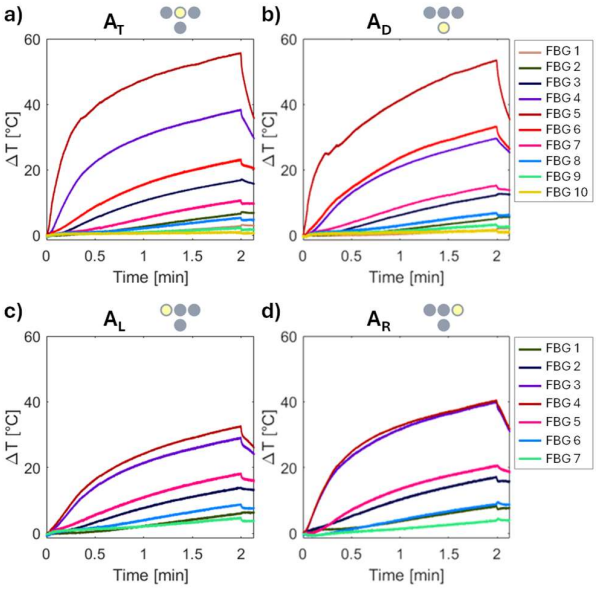

Figure 4. Temperature variation trends as function of time recorded by the arrays A_T (a), A_D (b), A_L (c), and A_R (d) during one of the experimental tests performed with NP_3. The symbol next to the title of each plot denotes the spatial position of the corresponding array (in yellow) with respect to the others.

As can be inferred from the reported trends, the FBG 5 of array A_T recorded the maximum temperature values, i.e., 55.8 °C, followed by FBG 5 of A_D, FBG 4 of A_L, and FBG 4 of A_R recording 53.7 °C, 32.8 °C, and 40.7 °C respectively. Indeed, the maximum temperature increment occurs nearby the laser fiber tip, and moving away from it the temperature quickly decreases.

4. Conclusions

Integration of NPs into laser ablation process and thermometry based on FBGs during this kind of treatment are gaining momentum in the last years both aiming to improve ablation selectivity in such a way as to prevent the risk of i) tumor recurrence and ii) healthy tissue thermal damage.

The study presented herein aims at developing novel NPs and investigating their effects on the temperature increase during in-vitro laser ablation tests on agarose-based phantoms. In particular, three kinds of polymer coated gold NPs each one showing surface plasmon resonance peak at a different wavelength have been tested. In order to perform accurate and reproducible tests, 34 FBGs have been located nearby the laser applicator and a custom 3D printed holder for shaping the phantom and positioning the fibers for laser and FBGs has been developed. A comparison among the different typologies of synthesized NPs has been carried out by assessing temperature trends in the target region. The experimental results highlight that by passing from the NPs absorbing at 700 nm to the ones absorbing at 970 nm, namely when the absorbing peak of the employed NPs approaches the laser wavelength, i.e., 1064 nm, a more significant temperature increment can be recorded. Indeed, with NP_1 the maximum ΔT values measured by each array range from 15.7 °C to 33.4 °C, whereas by using NP_3 maximum ΔT values range from 35.6 °C to 51.5 °C.

Future investigations will include the optimization and comparison among different structures of NPs in terms of treatment effects and the integration with numerical tools for simulating and better understanding the involved phenomena and to predict the treatment outcomes, moving towards an optimized and customized laser ablation.

5. Acknowledgements

This work was supported by the Italian Ministry of Education and Research through the project “MORE CARE”, CUP: I63C21000250006, under PRIN 2020 grant.

References

[1] E. De Vita, D. Lo Presti, C. Massaroni, A. Iadicicco, E. Schena, S. Campopiano, "A review on radiofrequency, laser, and microwave ablations and their thermal monitoring through fiber Bragg gratings", *IScience*, 26, 2023, pp. 108260, doi: 10.1016/j.isci.2023.108260.

[2] R.L. Manthe, S.P. Foy, N. Krishnamurthy, B. Sharma, V. Labhasetwar, "Tumor Ablation and Nanotechnology", *Mol. Pharm.*, 7, 2010, pp. 1880–1898, doi: 10.1021/mp1001944.

[3] S.R. Guntur, K. Il Lee, D.-G. Paeng, A.J. Coleman, M.J. Choi, "Temperature-Dependent Thermal Properties of ex Vivo Liver Undergoing Thermal Ablation", *Ultrasound Med. Biol.*, 39, 2013, pp. 1771–1784, doi: 10.1016/j.ultrasmedbio.2013.04.014.

[4] D. Germain, P. Chevallier, A. Laurent, H. Saint-Jalmes, "MR monitoring of tumour thermal therapy", *Magma Magn. Reson. Mater. Physics, Biol. Med.*, 13, 2001, pp. 47–59, doi: 10.1007/BF02668650.

[5] J. Chen, B. Liu, H. Zhang, "Review of fiber Bragg grating sensor technology", *Front. Optoelectron. China*, 4, 2011, pp. 204–212, doi: 10.1007/s12200-011-0130-4.

[6] M. Zaltieri, E. De Vita, F. De Tommasi, C. Massaroni, E. Faiella, B.B. Zobel, A. Iadicicco, E. Schena, R.F. Grasso, S. Campopiano, "Evaluation of the Thermal Response of Liver Tissue Undergoing Microwave Treatment by Means of Fiber Bragg Grating Sensors", *2020 IEEE SENSORS, IEEE*, 2020, pp. 1–4, doi: 10.1109/SENSORS47125.2020.9278851.

[7] Y. Bayazitoglu, S. Kheradmand, T.K. Tullius, "An overview of nanoparticle assisted laser therapy", *Int. J. Heat Mass Transf.*, 67, 2013, pp. 469–486, doi: 10.1016/j.ijheatmasstransfer.2013.08.018.

[8] P. Das, P. Fatehbasharzad, M. Colombo, L. Fiandra, D. Prosperi, "Multifunctional Magnetic Gold Nanomaterials for Cancer", *Trends Biotechnol.*, 37, 2019, pp. 995–1010, doi: 10.1016/j.tibtech.2019.02.005.

[9] Z. Ashikbayeva, D. Tosi, D. Balmassov, E. Schena, P. Saccomandi, V. Inglezakis, "Application of Nanoparticles and Nanomaterials in Thermal Ablation Therapy of Cancer", *Nanomaterials*, 9, 2019, pp. 1195, doi: 10.3390/nano9091195.

[10] P. Das, M. Colombo, D. Prosperi, "Recent advances in magnetic fluid hyperthermia for cancer therapy", *Colloids Surfaces B Biointerfaces*, 174, 2019, pp. 42–55, doi: 10.1016/j.colsurfb.2018.10.051.

[11] Q. Zhang, W. Li, L. Wen, J. Chen, Y. Xia, "Facile Synthesis of Ag Nanocubes of 30 to 70 nm in Edge Length with CF 3 COOAg as a Precursor", *Chem. – A Eur. J.,* 16, 2010, pp. 10234–10239, doi: 10.1002/chem.201000341.

[12] C.V.N. Bhaskar, S. Pal, P.K. Pattnaik, "Recent advancements in fiber Bragg gratings based temperature and strain measurement", *Results Opt.*, 5, 2021, pp. 100130, doi: 10.1016/j.rio.2021.100130.

[13] M. Nikfarjam, C. Christophi, "Interstitial laser thermotherapy for liver tumours", *Br. J. Surg.*, 90, 2003, pp. 1033–1047, doi: 10.1002/bjs.4326.